Molecular Pharmacology Fast Forward. Published on October 8, 2019 as DOI: 10.1124/mol.119.117234
This article has not been copyedited and formatted. The final version may differ from this version.

MOL# 117234

N-Terminal modification of the tetrapeptide Arg-Leu-Tyr-Glu, a VEGFR-2 antagonist, improves anti-tumor activity by increasing its stability against serum peptidases

Jung-A Yun[1], Joohwan Kim[1], Yi-Yong Baek[1], Wonjin Park, Minsik Park, Suji Kim, Taesam Kim, Seunghwan Choi, Dooil Jeoung, Hansoo Lee, Moo-Ho Won, Ji-Yoon Kim, Kwon-Soo Ha, Young-Guen Kwon, Young-Myeong Kim*

Departments of Molecular and Cellular Biochemistry (J-.A.Y., J.K., Y-.Y.B., W.P., M.P., S.K., T.K., S.C., K-.S.H., Y-.M.K.) and Neurobiology (M-.H.W.), School of Medicine Kangwon National University, Chuncheon, Gangwon-do, South Korea; Departments of Biochemistry (D.J.) and Life Sciences (H.L.), College of Natural Sciences, Kangwon National University, Chuncheon, Gangwon-do, South Korea; Kangwon Institute of Inclusive Technology, Kangwon National University, Chuncheon, Gangwon-do, South Kore (J.K., Y-.M.K.); Department of Anesthesiology and Pain Medicine, Hanyang University Hospital, Seoul, South Korea (J-,Y.K.); and Department of Biochemistry, College of Life Science and Biotechnology, Yonsei University, Seoul, South Korea (Y-.G.K.)

[1]These authors contributed equally to this article.

Running title: Serum stabilization of the VEGFR-2 antagonist RLYE

***Corresponding Author**. Department of Molecular and Cellular Biochemistry, School of Medicine, Kangwon National University, Chuncheon, Gangwon-do, 200-702, South Korea.
E-mail: ymkim@kangwon.ac.kr

Molecular Pharmacology Fast Forward. Published on October 8, 2019 as DOI: 10.1124/mol.119.117234
This article has not been copyedited and formatted. The final version may differ from this version.

MOL# 117234

Number of Pages: 33

Number of Tables: 0

Number of Figures: 7 + 1 supplemental

Number of References: 49

Number of words in Abstract: 234

Number of words in Introduction: 543

Number of words in Discussion: 1797

Abbreviations

Ac-RLYE, N-terminally acetylated RLYE; Arg1, arginase 1; CPT-11, irinotecan; EDTA, ethylenediaminetetraacetic acid; FBS, fetal bovine serum; HUVECs, human umbilical vein endothelial cells; iNOS, inducible nitric oxide; NG2; neural/glial antigen 2; PMSF, phenylmethylsulfonyl fluoride; RLYE, Arg-Leu-Tyr-Glu; RLYE-NH2, C-terminally amidated RLYE; VEGF, vascular endothelial growth factor; VEGFR-1/2/3, vascular endothelial growth factor receptor-1/2/3

Molecular Pharmacology Fast Forward. Published on October 8, 2019 as DOI: 10.1124/mol.119.117234
This article has not been copyedited and formatted. The final version may differ from this version.

Abstract

The tetrapeptide Arg-Leu-Tyr-Glu (RLYE), a vascular endothelial growth factor (VEGF) receptor-2 antagonist, has been used previously either alone or in combination with chemotherapeutic drugs for treating colorectal cancer in a mouse model. We analyzed the half-life of the peptide and found that due to degradation by aminopeptidases B and N, it had a short half-life of 1.2 h in the serum. Therefore, to increase the stability and potency of the peptide, we designed the modified peptide, N-terminally acetylated RLYE (Ac-RLYE), which had a strongly stabilized half-life of 8.8 h in serum compared with the original parent peptide. The IC_{50} value of Ac-RLYE for VEGF-A-induced endothelial cell migration decreased to approximately 37.1 pM from 89.1 pM for the parent peptide. Using a mouse xenograft tumor model, we demonstrated that Ac-RLYE was more potent than RLYE in inhibiting tumor angiogenesis and growth, improving vascular integrity and normalization through enhanced endothelial cell junctions and pericyte coverage of the tumor vasculature, and impeding the infiltration of macrophages into tumor and their polarization to the M2 phenotype. Furthermore, combined treatment of Ac-RLYE and irinotecan exhibited synergistic effects on M1-like macrophage activation and apoptosis and growth inhibition of tumor cells. These findings provide evidence that the N-terminal acetylation augments the therapeutic effect of RLYE in solid tumors via inhibition of tumor angiogenesis, improvement of tumor vessel integrity and normalization, and enhancement of delivery and efficacy of the co-administered chemotherapeutic drugs.

Molecular Pharmacology Fast Forward. Published on October 8, 2019 as DOI: 10.1124/mol.119.117234
This article has not been copyedited and formatted. The final version may differ from this version.

Significant statement: The results of this study demonstrate that the N-terminal acetylation of the tetrapeptide RLYE (Ac-RLYE), a novel VEGFR-2 inhibitor, significantly improves its serum stability, anti-angiogenic activity, and vascular normalizing potency, resulting in enhanced therapeutic effect on solid tumors. Furthermore, the combined treatment of Ac-RLYE with the chemotherapeutic drug, irinotecan, synergistically enhanced its anti-tumor efficacy by improving the perfusion and delivery of the drug into the tumors and stimulating the conversion of the tumor-associated macrophages to an immunostimulatory M1-like anti-tumor phenotype.

1. Introduction

Tumor angiogenesis improves the formation of blood vessels for supplying oxygen, nutrients, and growth factors required for the growth and survival of tumors (Folkman, 2007). This process is initiated from pre-existing vasculature around the tumors (Folkman, 2007; Papetti and Herman, 2002). Angiogenesis is precisely regulated by a balance between the pro- and anti-angiogenic factors. Among the various angiogenic factors, vascular endothelial growth factor (VEGF), which is predominantly induced under hypoxic conditions including robust tumor growth, is identified as the most potent and prominent factor to induce physiological and pathological neovascularization through the activation of endothelial cells (Papetti and Herman, 2002). Thus, VEGF contributes to tumor progression by promoting angiogenesis (Folkman, 2007).

The VEGF family includes five VEGF isoforms (VEGF-A, VEGF-B, VEGF-C, VEGF-D, and VEGF-E) and placental growth factor (Hicklin and Ellis, 2005). Of these, VEGF-A is the most potent inducer of angiogenesis. All the VEGF isoforms bind to the receptor tyrosine kinases, VEGF receptor-1 (VEGFR-1), VEGFR-2, and VEGFR-3. However, VEGF-A binds to and activates both VEGFR-1 and VEGFR-2, which are expressed mainly in endothelial cells. VEGFR-1 has a higher binding affinity for VEGF-A compared to VEGFR-2, whereas its angiogenic activity is much weaker than that of VEGFR-2 (Sawano et al., 1996). Therefore, the VEGF-A/VEGFR-2 pathway is the main axis driving angiogenesis under physiological and pathological conditions.

Numerous studies have demonstrated that antibodies and chemical drugs targeting the VEGF-A/VEGFR-2 axis are potential strategies to inhibit tumor angiogenesis, thus abrogating tumor progression and metastasis. Although some of them, such as bevacizumab, ramucirumab, sunitinib, and axitinib, have been clinically used to treat several solid tumors

Molecular Pharmacology Fast Forward. Published on October 8, 2019 as DOI: 10.1124/mol.119.117234
This article has not been copyedited and formatted. The final version may differ from this version.

(McIntyre and Harris, 2015), they have some limitations due to unwanted adverse effects (Kamba and McDonald, 2007; Taugourdeau et al., 2012; Cook and Figg, 2010; Verheul and Pinedo, 2007). For example, the anti-VEGF-A antibody bevacizumab frequently induces serious side effects, including severe hypertension, thromboembolic events, bleeding, and hemorrhage in cancer patients (Kamba and McDonald, 2007; Taugourdeau et al., 2012). In addition, chemical drugs that inhibit VEGF receptor tyrosine kinase can inhibit several other tyrosine kinases due to their low specificity and can also lead to drug-resistance, hypertension, and proteinuria (Cook and Figg, 2010; Verheul and Pinedo, 2007). However, the anti-VEGFR-2 antibody ramucirumab is predicted to be a promising drug for treating cancer patients, since it inhibits tumor angiogenesis without significant adverse effects (Javle et al., 2014; Fuchs et al., 2014), suggesting that VEGFR-2 could be a potential target for tumor therapy.

We had previously developed the anti-angiogenic tetrapeptide Arg-Leu-Tyr-Glu (RLYE) from the amino acid sequence of Lys-Leu-Tyr-Asp (KLYD) present in the anti-angiogenic kringle domain 5 of plasminogen (Baek et al., 2015; Sheppard et al. 2004). RLYE inhibited VEGF-induced angiogenesis *in vitro* more effectively than KLYD (Baek et al., 2015). Further studies demonstrated that RLYE acts as a VEGFR-2 antagonist and inhibits tumor angiogenesis by binding to VEGFR-2 at the same binding site as VEGF-A (Baek et al., 2015; Baek et al., 2017). Here, we found that RLYE had a short half-life in serum and therefore, we developed a more stable peptide, Ac-RLYE, by N-terminal acetylation of RLYE. The modified peptide potentially inhibited tumor angiogenesis and improved tumor vessel integrity in an animal model. These findings provide evidence that Ac-RLYE is a promising therapeutic drug for solid tumors by targeting tumor vessels.

2. Materials and Methods

2.1. Materials

Cell culture media and supplements were purchased from Invitrogen Life Technologies (Carlsbad, CA, USA). Fetal bovine serum (FBS) was obtained from HyClone Laboratories (Logan, UT, USA). Human recombinant VEGF-A_{165} was obtained from R&D Systems (Minneapolis, MN, USA). The peptides RLYE, Ac-RLYE, and other peptides were purchased from Peptron (Daejeon, South Korea). Irinotecan hydrochloride (CPT-11) was purchased from Sigma-Aldrich (St. Louis, MO, USA). Aprotinin, leupeptin, ethylenediaminetetraacetic acid (EDTA), and phenylmethylsulfonyl fluoride (PMSF) were purchased from Thermo Fisher Scientific (Waltham, MA, USA). Bestatin, arphamenine B, and leuhistin were obtained from Calbiochem (San Diego, CA, USA).

2.2. Cell culture

Human HCT116 colon cancer cells and human umbilical vein endothelial cells (HUVECs) were obtained from American Type Culture Collection (Manassas, VA, USA) and ScienCell Research Laboratories (San Diego, CA, USA), respectively. HCT116 cells were cultured in RPMI medium supplemented with 10% FBS, 1 mM sodium pyruvate, 10 mM 4-(2-hydroxyethyl)-1-piperazineethanesulfonic acid, and 100 U/ml penicillin-streptomycin antibiotic solution in a humidified atmosphere of 5% CO_2 at 37°C. HUVECs were maintained and cultured in M199 as previously described (Baek et al., 2017), and only passages 2-6 were used for all experiments.

2.3. *In vitro* angiogenesis assay

Angiogenic activity was determined by measurements of endothelial cell migration and tube formation as described previously (Baek et al., 2017). Chemotactic migration was analyzed

Molecular Pharmacology Fast Forward. Published on October 8, 2019 as DOI: 10.1124/mol.119.117234
This article has not been copyedited and formatted. The final version may differ from this version.

using Boyden chambers. Briefly, the lower surface of the filter of Boyden chambers with 6.5-mm-diameter polycarbonate filters (8 μm pore size) was coated with 10 μg of gelatin. Fresh M199 medium containing FBS (1%) and VEGF (10 ng/ml) was placed in the lower wells. HUVECs were trypsinized and resuspended at a final concentration of 1×10^6 cells/ml in M199 containing FBS (1%) and peptides (1.5 nM or 1 pM-10 nM). The cell suspension was added into each of the upper wells in a final volume of 100 μl. After incubation at 37ºC for 4 h, the cells that migrated to the lower side of the filter were fixed and stained with hematoxylin and eosin and counted using a phase-contrast microscope. On the other hand, the formation of tube-like structure was determined following culture of HUVECs on growth factor reduced Matrigel (Baek et al., 2017). Twenty-four well culture plates were coated with Matrigel according to the manufacturer's instructions. HUVECs were plated onto the layer of Matrigel at a density of 4.0×10^5 cells/well and stimulated with VEGF (10 ng/ml) alone or in combination with the peptides (1.5 nM) pre-incubated with either phosphate-buffered saline (PBS) or fresh human serum for 2 h. After 20 h, the tube-like structure formation was visualized using a phase-contrast inverted microscope (Olympus IX71, Tokyo, Japan). The degree of tube formation was quantified using ImageJ software (NIH, Bethesda, MA, USA).

2.4. Determination of peptide degradation and stability

Human whole blood was collected in sterile centrifuge tubes from healthy volunteers according to protocols approved by the Institutional Review Board at Kangwon National University Hospital (KNUH-2017-01-010-004), and informed consent was obtained from all participants. The investigation conforms to the principles outlined in the Declaration of Helsinki. Whole blood was allowed to clot at 4°C and then centrifuged at 1500 × *g* for 20 min at 4°C. The serum was filtered with a sterile filter (0.22 μm, Millipore Corporation, Billerica, MA, USA) and

stored in small aliquots at -70°C until further use. For measuring the stability of each peptide in serum, the peptides (100 μg in 50 μl of distilled water) were incubated with 50 μl of filtered human serum in the presence or absence of protease or peptidase inhibitors in a 37°C incubator for the indicated periods. The incubated sample was fractionated by reverse-phase C18 high-performance liquid chromatography (HPLC) with a linear gradient of acetonitrile (Vydac protein and peptide C18 Column, 0.1% trifluoroacetate in H_2O for equilibration, and 0.1% trifluoroacetate in acetonitrile for elution). The relative concentrations of the remaining peptides were analyzed by integration of the absorbance at 220 nm as a function of retention time using the Analysis module of the Unicorn software package.

2.5. Animal model of human colon cancer

Seven-week-old male athymic nude mice were purchased from OrientBio (Seongnam, South Korea) and maintained on a standard chow diet *ad libitum* in a laminar airflow cabinet under specific pathogen-free conditions. Animal experiments were performed in accordance with the guidelines of the Institutional Animal Care and Use Ethics Committee of Kangwon National University (KW-181109-1). Moreover, this investigation conformed to the Guide for the Care and Use of Laboratory Animals published by the United States National Institutes of Health (NIH Publications No. 8023, revised 1978). The sample size for animal experiments was determined according to a previously modified method using a G power program (Charan and Kantharia, 2013). Nude mice were randomly allocated to experimental and control groups and challenged subcutaneously (s.c.) in the left flank with 100 μl of 1×10^7 HCT116 human colon carcinoma cells. After the tumor volume grew to at least 50-70 mm^3, which occurred within 7 days, the mice were injected intraperitoneally (i.p.) with saline, RLYE (0.5 mg/kg daily), or modified RLYE (0.5 mg/kg daily). Some mice were i.p. injected with Ac-RLYE (0.5

mg/kg daily), RLYE (0.5 mg/kg daily), or in combination with CPT-11 (17 mg/kg every 5 days). The dosage of CPT-11 is one-third of the maximum-tolerated dose (50 mg/kg every 3 days) in the tumor-bearing mouse model and does not induce cytotoxicity when injected intraperitoneally every 3 days (Uchino et al., 2008). The tumor size was measured in two dimensions using calipers. The tumor volume (mm^3) was calculated using the ellipsoid formula: $width^2 \times length \times 0.52$ (Baek et al., 2017).

2.6. Tumor vessel permeability

Tumor vessel permeability was assessed using fluorescein isothiocyanate (FITC)-dextran as previously described (Baek et al., 2017). The tumor-bearing mice were treated with peptides alone or in combination with CPT-11 for 18 days and then intravenously (i.v.) injected with 3 mg/mouse FITC-dextran (40 kDa; Sigma-Aldrich, St. Louis, MO, USA). After 10 min, the tumors were isolated and fixed briefly in 4% paraformaldehyde, and cryosections of the tumor tissues were prepared to observe vascular leakage under a fluorescence microscope.

2.7. Immunostaining analysis

The tumor tissues were fixed in 3.7% paraformaldehyde solution overnight at 4°C, rinsed with PBS at room temperature, incubated in 15% sucrose overnight at 4°C, and transferred to 30% sucrose at 4°C until the tissue sank. The fixed tissues were embedded in Optimal Cutting Tissue compound (Leica Biosystems, Richmond, IL, USA) for 30 min at room temperature and subsequently frozen in liquid nitrogen. Frozen sections (30 μm thick) were cut at -20℃, and the slides were stored at -70°C until they were used for immunostaining. The sections were incubated with antibodies for rat anti-CD31 (1:100, #553370, DB Pharmingen, San Jose, CA, USA), inducible nitric oxide (iNOS, 1:100, #610600), goat anti-VE-cadherin (1:100, Santa

Cruz Biotechnology, Santa Cruz, SC-9989, CA, USA), arginase 1 (1:100, Arg1, SC-166920), F4/80 (1:100, SC-26642), and rabbit anti-NG2 (1:500, ab5320, EMD Millipore, Billerica, MA, USA) for 2 h at room temperature. After washing 3 times with 0.1% Triton X-100 in PBS (10 min/wash), the sections were incubated with Alexa Fluor-, FITC-, or tetramethylrhodamine-isothiocyanate (TRITC)-conjugated secondary antibody (1:1000) for 60-90 min at room temperature, counterstained with DAPI (1 μg/ml) and washed 5 more times with 0.1% Triton X-100 solution (10 min/wash). Some of the tumor sections were also incubated with FITC-isolectin B4 (5 μg/ml; Vector Laboratories, Burlingame, CA, USA) for 1 h. In addition, the apoptotic cells were detected using a terminal deoxynucleotidyl transferase dUTP nick end labeling (TUNEL) kit (Roche Applied Science, Indianapolis, IN, USA). The slides were mounted with Permount solution (Thermo Fisher Scientific, Waltham, MA, USA) and analyzed using the Zeiss LSM 880 laser scanning confocal microscope with AiryScan (Carl Zeiss, Oberkochen, Germany). Images were acquired with pinhole settings of 1 Airy Unit, on a GaAsP-PMT detector with a gain setting of 800, a pixel dwell time of 2.06 μs, and no averaging. Airyscan images were acquired with 2% of maximum laser power for argon-ion (488 nm), helium-neon (633 and 543 nm), and diode (405 nm) laser lines. The image acquisition parameters were kept constant between the control and treated groups. Colocalization of CD31 and VE-cadherin was assessed by Pearson's correlation coefficient using the ZEN software in a blinded investigation.

2.8. Statistical analysis

The quantitative data are expressed as mean ± standard deviation (SD) of at least three independent experiments performed in triplicate. Image analysis was performed by three blinded observers, and no samples were excluded from the analysis. Statistical analyses were

performed using GraphPad Prism 6 (La Jolla, San Diego, CA, USA). Statistical significance was determined using either the unpaired student's *t*-test or one-way ANOVA followed by Tukey's post-hoc test, depending on the number of experimental groups analyzed. Differences were considered statistically significant at $P < 0.05$. For all statistical analyses, the appropriate statistical tests were chosen, and the data met the assumptions of the test and the variance between the statistically compared groups was similar.

3. Results

3.1. RLYE is degraded by heat-labile serum factors.

Since small peptides are likely to be unstable in the serum due to the presence of serum-derived peptidases and therefore rapidly cleared from blood circulation, we first examined the stability of the VEGFR-2 antagonist RLYE (structure shown in Fig. 1A) in fresh human serum using HPLC-based spectrophotometry following incubation for different time periods at 37°C. The characteristic peak of RLYE was rapidly reduced in the serum with a half-life ($t_{1/2}$) of 73 min, while it was quite stable in PBS (Fig. 1B), suggesting that this peptide is degraded or absorbed by certain biomolecules present in the serum. We next examined whether the stability of the peptide was affected by heat-labile serum factors, such as peptidases or proteases. The serum was preheated at different temperatures for 10 min and incubated with RLYE for 2 h, followed by quantitation of the amount of the remaining peptide. The peptide stability remained unchanged only when incubated with serum preheated over 70°C (Fig. 1C). These data suggest that RLYE may be degraded or destabilized by heat-labile serum factors.

3.2. RLYE is degraded by aminopeptidases B and N.

Since enzymes are generally neutralized by heating over about 70°C, we examined the identity of the proteins, including enzymes, which are involved in the degradation or destabilization of RLYE. When incubated with albumin, the most abundant protein in serum, RLYE remained stable (Fig. 2A), indicating that the stability of RLYE is not affected by albumin. However, co-incubation with protease inhibitors, such as aprotinin, leupeptin, PMSF, or EDTA, failed to restore the decreased peak height of RLYE that was observed upon incubation with serum (Fig. 2A), suggesting that serum proteases are not involved in the destabilization of RLYE. Based on the amino acid sequence of the peptide, we hypothesized that aminopeptidases B and N, which cleave Arg at the N-terminal residue, may contribute to the degradation of RLYE. Notably, bestatin, an inhibitor of aminopeptidases B and N completely restored the decreased peak height of RLYE incubated with serum (Fig. 2B). These results suggest that aminopeptidases B and N are responsible for degradation of RLYE in the bloodstream. We next examined which of these aminopeptidases is predominantly involved in the destabilization of RLYE in serum using their specific inhibitors. Destabilization of RLYE in serum was partially inhibited by both aminopeptidase B-specific inhibitor (arphamenine B) and N-specific inhibitor (leuhistin), and the inhibitory effect of leuhistin was slightly higher than that of arphamenine B. However, combined treatment with both inhibitors completely blocked the destabilization of RLYE in serum (Fig. 2C). These results suggest that RLYE is degraded by both serum aminopeptidases B and N.

3.3. N-terminal modification stabilizes RLYE and potentiates its anti-angiogenic activity.

To improve the stability of the peptide from serum peptidase-mediated degradation, RLYE was modified at either the N- or C-terminal residue. N-terminal acetylation (Ac-RLYE)

Molecular Pharmacology Fast Forward. Published on October 8, 2019 as DOI: 10.1124/mol.119.117234
This article has not been copyedited and formatted. The final version may differ from this version.

significantly increased the half-life of RLYE (1.2 h) to approximately 8.8 h in fresh serum, whereas the C-terminal amidation (RLYE-NH_2) did not effectively change the serum stability of RLYE (Fig. 3, A and C). Similar to Ac-RLYE, $R_{(D)}$LYE, in which L-Arg of RLYE is replaced with its inactive stereoisomer D-Arg, also had an increased serum half-life of 7.0 h compared with that of RLYE, indicating that $R_{(D)}$LYE is stable in serum, albeit slightly less compared with Ac-RLYE (Fig. 3, B and C). However, modification of RLYE at both N- and C-termini (Ac-RLYE-NH_2) increased its serum half-life to 9.4 h, which was slightly longer than that of Ac-RLYE and much longer than that of RLYE-NH_2 (Fig. 3C). This suggests that the N-terminal L-Arg residue is a critical determinant of the stability of RLYE in serum. We next examined the effects of RLYE and its modified versions on VEGF-A-induced endothelial migration, which is a typical characteristic of *in vitro* angiogenesis. Treatment of HUVECs with 1.5 nM of Ac-RLYE and $R_{(D)}$LYE showed slightly higher inhibitory effects of 95.8% and 91.4%, respectively, than RLYE (85.4%) on VEGF-A-induced endothelial cell migration; however, RLYE-NH_2 revealed lower inhibitory effect (79.7%) than RLYE (Fig. 3C). On the other hand, Ac-RLYE-NH_2 had a significantly lower inhibitory effect on VEGF-A-induced endothelial cell migration compared with that of RLYE (11.3 vs. 85.4%). To further compare the anti-angiogenic activities of all the peptides, the IC_{50} values were determined against VEGF-A-induced endothelial cell migration. The IC_{50} values of Ac-RLYE and $R_{(D)}$LYE were approximately 37.1 pM (95% confidence interval (CI): 69.1-44.7 pM) and 52.5 pM (95% CI: 39.8-70.8), respectively, which were lower than that of RLYE (IC_{50}: 89.1 pM, 95% CI: 69.1-116.9 pM). However, the IC_{50} values of RLYE-NH_2 and Ac-RLYE-NH_2 were 326.6 pM (95% CI: 224.8-475.3 pM) and >1.0 nM, respectively, which were much higher than that of RLYE (Fig. 3C; Supplementary Fig. 1). Furthermore, we compared the anti-angiogenic activity of the peptides following pre-incubation with PBS or human serum for 2 h, to mimic the *in vivo*

Molecular Pharmacology Fast Forward. Published on October 8, 2019 as DOI: 10.1124/mol.119.117234
This article has not been copyedited and formatted. The final version may differ from this version.

system of circulating blood. When pre-incubated either with PBS or human serum, $R_{(D)}$LYE and Ac-RLYE strongly inhibited VEGF-induced tube-like structure formation, whereas RLYE had potent anti-angiogenic activity when pre-incubated with PBS but showed only partial activity with human serum (Fig. 3D), suggesting that $R_{(D)}$LYE and Ac-RLYE have more potent anti-angiogenic activity than RLYE in serum. Collectively, our results suggest that the N-terminal modification greatly stabilizes RLYE in circulating blood and effectively inhibits VEGF-A-induced angiogenesis.

3.4. Ac-RLYE and $R_{(D)}$LYE potentially inhibit tumor growth and angiogenesis.

We examined the anti-tumor effects of Ac-RLYE and $R_{(D)}$LYE in a human colorectal tumor xenograft model. Treatment with both modified peptides significantly inhibited tumor growth and decreased tumor size and weight compared with RLYE treatment, and the anti-tumor effects of Ac-RLYE were slightly greater than those of $R_{(D)}$LYE (Fig. 4, A-C). We next assessed the inhibitory effects of these peptides on tumor angiogenesis. Immunohistochemical analysis of CD31, an endothelial specific marker, showed that both modified peptides significantly decreased blood vessel formation in the tumor tissues compared with RLYE, and the effect of Ac-RLYE was greater than that of $R_{(D)}$LYE (Fig. 4, D and E). Therefore, these data suggest that Ac-RLYE has more a potent anti-tumor effect than the other peptides via effective inhibition of tumor angiogenesis.

3.5. Ac-RLYE improves normalization of tumor vessels.

Since tumor angiogenesis forms the abnormal vasculature in conjunction with increased vascular permeability and leakage, leading to tumor progression and metastasis (Jain, 2005), we evaluated the effect of Ac-RLYE on the vascular permeability and leakage in tumors using

Molecular Pharmacology Fast Forward. Published on October 8, 2019 as DOI: 10.1124/mol.119.117234
This article has not been copyedited and formatted. The final version may differ from this version.

FITC-dextran. Treatment of tumor-bearing mice with Ac-RLYE significantly reduced tumor vessel leakage compared with that of saline control, and this effect was greater than that of RLYE (Fig. 5, A and B). Vascular permeability has been known to be regulated by abnormal vascular structures, such as loss of endothelial cell junctions and lack of pericytes (Hellström et al., 2001). As expected, we found that treatment with Ac-RLYE resulted in a high degree of colocalization of CD31 and VE-cadherin, an endothelial cell junction protein, as well as a significant decrease in CD31 immunoreactivity compared with RLYE treatment (Fig. 5, C and D). Moreover, Ac-RLYE treatment resulted in increased pericyte coverage on tumor vessels compared with RLYE treatment, as determined by staining with the pericyte marker NG2 (Ozerdem et al., 2001) (Fig. 5, E and F). These results suggest that the N-acetylation improves the effect of RLYE on tumor vessel normalization through enhancement of endothelial cell junctions and pericyte coverage.

3.6. Ac-RLYE sensitizes tumor to CPT-11.

Since reduced vascular leakage via tumor vessel normalization increases drug delivery to solid tumors and facilitates chemotherapeutic efficacy (Jain, 2005; Carmeliet and Jain, 2011; Dineen et al., 2008), we examined the combined effect of the peptides and an anticancer drug CPT-11 (17 mg/kg every 5 days) on tumor progression. Co-treatment with RLYE and CPT-11 revealed a synergistic inhibition of tumor growth, and this synergistic effect was further augmented by replacement of RLYE with Ac-RLYE (Fig. 6A). Consistent with this, TUNEL assay showed that apoptotic cells were synergistically augmented in tumors of mice treated with a combination of Ac-RLYE and CPT-11, and the synergistic apoptosis was greater than that induced by co-treatment with RLYE and CPT-11 (Fig. 6, A-C). However, treatment with Ac-RLYE, CTP-11, and both together did not significantly change the serum levels of the

hepatotoxicity markers alanine aminotransferase and aspartate aminotransferase (Fig. 6D) and the body weights (23.5 ± 0.8, 24.1 ± 0.8, and 22.8 ± 0.7 g, respectively), in concordance with the results shown in a previous study (Uchino et al., 2008). These results suggest that the N-acetylation enhances the effect of RLYE on CPT-11-mediated chemotherapeutic efficacy without significant toxicity in a mouse model.

3.7. Ac-RLYE inhibits infiltration of macrophages and their polarization to M2 phenotype.

Tumor-associated macrophages (TAMs) express VEGFR-2 (Dineen et al., 2008) and play an important role in tumor angiogenesis by polarization from the cytotoxic M1 to the angiogenic M2 phenotype (Riabov et al., 2014). We examined whether Ac-RLYE regulates infiltration of macrophages into tumors and their phenotypic polarization. Treatment with Ac-RLYE significantly decreased infiltration of F4/80-positive macrophages into tumors compared with injection of saline (Fig. 7, A and B). TAMs in mice treated with Ac-RLYE expressed low levels of the M2 macrophage marker Arg1 and high levels of the M1 macrophage marker iNOS compared with TAMs in saline-treated mice (Fig. 7, A, C, D, and E). CPT-11 treatment resulted in a significant increase in infiltration of macrophages, which expressed high levels of Arg1 and low levels of iNOS compared with those in control tumors, and these gene expression patterns were inversely regulated by co-treatment with Ac-RLYE (Fig. 7, A, C, D, and E). Therefore, treatment with Ac-RLYE inhibited infiltration of macrophages and polarization of TAMs to the M2 phenotype (Fig. 7, B and F), possibly resulting in an increase in TAM-induced tumor cytotoxicity.

4. Discussion

Molecular Pharmacology Fast Forward. Published on October 8, 2019 as DOI: 10.1124/mol.119.117234
This article has not been copyedited and formatted. The final version may differ from this version.

Since formation of the tumor vascular network plays a critical role in tumor growth and metastasis, many angiogenic inhibitors have been developed and clinically used for treating solid tumors (McIntyre and Harris, 2015; Kamba and McDonald, 2007; Taugourdeau et al., 2012; Cook and Figg, 2010; Verheul and Pinedo, 2007). The tumor vasculature created by tumor-derived VEGF exhibits a spectrum of morphological and functional abnormalities characterized by loss of vessel hierarchy, increased tortuosity, poor perfusion, instability, and increased vascular leakage (McDonald and Baluk, 2005). Thus, anti-angiogenic agents not only inhibit tumor angiogenesis, but also normalize the tumor vasculature, resulting in improved chemotherapeutic efficacy by enhancing the delivery of anticancer drugs to tumors.

We previously demonstrated that the tetrapeptide RLYE effectively suppressed tumor neovascularization by blocking the interaction between VEGF-A and VEGFR-2, resulting in inhibition of tumor growth and metastasis in a tumor-bearing mouse model (Baek et al., 2015; Baek et al., 2017). However, we found that RLYE was unstable and readily degraded with a half-life of approximately 1.2 h when incubated in human serum. This short half-life was due to serum aminopeptidases B and N, which cleave the N-terminal Arg residue of the peptide. Since these enzyme activities are elevated in the sera of patients with breast and pancreatic cancer (Dineen et al., 2008; Martinez-Martos et al., 2011), RLYE would need to be modified to be resistant to both aminopeptidases for clinical use in tumor treatment. To address this need, we developed N-terminal modified peptides, Ac-RLYE and $R_{(D)}$LYE, with increased stability of 7.3 and 5.8 folds, respectively, in serum compared with RLYE. Ac-RLYE had more potent inhibitory activity than $R_{(D)}$LYE against VEGF-A-induced *in vitro* angiogenesis. Moreover, Ac-RLYE effectively inhibited tumor angiogenesis and tumor growth, as well as improved tumor vessel normalization, resulting in enhanced therapeutic efficacy when co-treated with the chemotherapeutic drug CPT-11. As demonstrated by clinical evidence that anti-angiogenic

agents show anti-tumor activity mostly in combination with chemotherapeutics (Sengupta et al., 2015; Margonis et al., 2017), our findings strongly suggest that Ac-RLYE could be used as a potential drug for anti-angiogenic tumor therapy or in combination with chemotherapy.

Tumor angiogenesis progresses from the preexisting normal vessels surrounding the tumor under the influence of pro-angiogenic growth factors secreted by the tumor cells. Among the angiogenic stimulators, the VEGF family are the most potent mitogenic and angiogenic activators (Hicklin and Ellis, 2005). Of the VEGF isoforms, VEGF-A is the most important factor controlling tumor angiogenesis and vascular network (Folkman, 2007; Papetti and Herman, 2002). VEGF-A binds to both VEGFR-1 and VEGFR-2, which are expressed mainly in endothelial cells. VEGFR-1 has a high binding affinity for VEGF-A, which is one order higher than that of VEGFR-2, whereas its angiogenic activity is approximately 10-fold weaker than that of VEGFR-2 (Sawano et al., 1996; Shibuya, 2011). Therefore, VEGFR-2 plays a crucial role not only in physiological angiogenesis during wound healing and embryogenesis, but also in pathological angiogenesis during tumor growth and metastasis (Kerbel, 2008). Thus, VEGFR-2 is a potential therapeutic target for inhibiting tumor angiogenesis and tumor progression (Roland et al., 2009). We previously demonstrated that RLYE interferes with the interaction between VEGF-A and VEGFR-2, leading to endothelial dysfunction. Since RLYE was rapidly degraded by serum-derived aminopeptidases B and N, we developed Ac-RLYE, a peptide with increased stability in serum, which inhibited tumor angiogenesis even more and improved the tumor vessel normalization.

RLYE binds specifically to VEGFR-2, but not VEGFR-1, at the interface between the immunoglobulin homology domains D2 and D3 (Baek et al., 2017), which is known to be the binding site for VEGF-A/C (Leppänen et al., 2010). Notably, both the terminal residues of RLYE, Arg and Glu, bind electrostatically to Glu140 and Lys286 of VEGFR-2, respectively,

Molecular Pharmacology Fast Forward. Published on October 8, 2019 as DOI: 10.1124/mol.119.117234
This article has not been copyedited and formatted. The final version may differ from this version.

and Lys286 is crucial for the formation of a salt bridge with Glu64 of VEGF-A (Leppänen et al., 2010). Ac-RLYE was stable in serum and increased anti-angiogenic activity, indicating that the N-terminal acetylation does not affect interaction between Ac-RLYE and VEGFR-2. On the other hand, RLYE-NH_2 was not stable in serum but partially decreased anti-angiogenic activity, while Ac-RLYE-NH_2 was more stable in serum compared with the other modified peptides but showed markedly decreased anti-angiogenic activity compared with RLYE. These phenomena can be explained by two possibilities. First, RLYE can be degraded not only by aminopeptidases B and N, but also partially by other enzymes, including glutamate carboxypeptidase, which is a secreted enzyme that hydrolyzes the C-terminal Glu of peptides in circulating blood (Lee et al., 2016). However, we cannot exclude another possibility that it can be destabilized by unknown endopeptidases, because half-life of Ac-RLYE-NH_2 was less than 10 h when incubated with serum. Second, both positive and negative charges at the termini of the peptide are important for its biological activity due to their essential contribution to interaction with VEGFR-2 (Baek et al., 2017; Leppänen et al., 2010). This structural and binding information is important for developing non-peptidic small molecules targeting VEGFR-2, with strong resistance to the blood peptidases.

Since tumor blood vessels are heterogeneous, tortuous, and irregularly branched, they are structurally and functionally abnormal (Jain, 2005). The tumor vessels are poorly perfused, hyperpermeable, and leaky with loss of inter-endothelial junctions and less coverage of pericytes, thereby limiting the delivery of cytotoxic agents to tumors and hence decreasing chemotherapeutic efficacy (Carmeliet and Jain, 2011). In general, anti-angiogenic drugs targeting the VEGF-A/VEGFR-2 system not only inhibit tumor angiogenesis, but also promote tumor vascular normalization, leading to an increase in drug delivery and efficacy when they are combined with chemotherapeutic drugs (Jain, 2005; Carmeliet and Jain, 2011; Dineen et

Molecular Pharmacology Fast Forward. Published on October 8, 2019 as DOI: 10.1124/mol.119.117234
This article has not been copyedited and formatted. The final version may differ from this version.

al., 2008). Others and we have demonstrated that combination therapy of the anti-angiogenic drug bevacizumab or vascular leakage blocker Sac-1004 with anticancer drugs increased drug delivery through tumor vessel normalization and hence improved the anti-tumor efficacy (Agrawal et al., 2014; Dickson et al., 2007; Yanagisawa et al., 2010). Similarly, we demonstrated that Ac-RLYE fostered vascular normalization through improvement of endothelial junctions and pericyte coverage, resulting in increased tumor cell apoptosis and therapeutic efficacy of co-administered CPT-11.

Accumulating evidence suggest that the VEGF-A/VEGFR-2 axis is also crucial for the immune modulation of the tumor microenvironment in addition to its effect on the vasculature (Dineen et al., 2008; Roland et al., 2009). The VEGF-A/VEGFR-2 axis is not only important for tumor vascularization, but is also a key factor in the inhibition of the recognition and destruction of tumor cells via negative regulation of the immune system (Ohm and Carbone, 2001). In fact, VEGF-A has been shown to interfere with cell-mediated immunity by decreasing differentiation, recruitment, function of T-cells, and development of T-cells from early hematopoietic progenitor cells in tumor-bearing mice and cancer patients (Ohm et al., 2003; Shrimali et al., 2010; Terme et al., 2013; Osada et al., 2008). A more interesting study showed that VEGF-A enhances the expression of PD-1 and other inhibitory checkpoints involved in $CD8^+$ T cell exhaustion (Voron et al., 2015). This suggests that inhibitors of the VEGF-A/VEGFR-2 axis play a key role in preventing the development of an immunosuppressive microenvironment. Therefore, selective inhibition of the activation of VEGFR-2 by treatment with the anti-VEGF-A antibody r84 can effectively restore anti-tumor immunity by decreasing infiltration of suppressive immune cells (myeloid-derived suppressor cells and Treg) and elevating a population of functionally mature dendritic cells within tumors compared with other anti-VEGF therapies (Roland et al., 2009). VEGF-A enhances infiltration of macrophages into

tumors via activation of VEGFR-2 (Wheeler et al., 2018), as well as stimulates the polarization of TAMs from the cytotoxic M1 to the angiogenic M2 phenotype (Riabov et al., 2014). M2 polarization contributes to a detrimental tumor microenvironment via VEGF expression and immune suppression (Mazibrada et al., 2008; Zhong et al., 2015). Therefore, treatment with anti-angiogenic drugs, including Ac-RLYE, that target the VEGF-A/VEGFR-2 axis is a useful regimen for promising outcomes by negatively regulating macrophage infiltration and polarization in preclinical and clinical settings (Dineen et al., 2008; Rivera and Bergers, 2015). Furthermore, recent studies demonstrated that the combination of anti-angiogenic drugs (bevacizumab and trebananib) and immune checkpoint inhibitors (ipilimumab and pembrolizumab) show promising therapeutic effects in patients with melanoma and renal cell cancer (Wu et al., 2017; Rahma and Hodi, 2019). This suggests that Ac-RLYE may be beneficial for combination therapy with immune checkpoint inhibitors. This possibility should be examined in the near future.

Many studies have demonstrated that the exposure of tumors to chemotherapeutic drugs increases infiltration of macrophages expressing the M2-marker MCR1 into tumor, leading to increased angiogenesis and limited chemotherapeutic efficacy, probably by increasing hypoxia-inducible factor-1α (HIF-1α)-dependent CXCL12 and VEGF expression (Zhao et al., 2017; Hughes et al., 2015). These results are consistent with our data showing an increase in M2-type macrophage infiltration in tumor-bearing mice receiving CPT-11. However, the CPT-11-induced increase in macrophage infiltration and M1/M2 polarization could be blocked or reprogrammed via tumor vessel normalization, decreased vascular leakiness, and favorable tumor environment (decreased HIF-1α level) by treatment with anti-angiogenic drugs, including Ac-RLYE (Baek et al., 2017; Dineen et al., 2008; De Palma and Lewis, 2013). Based on these results, combined therapy of Ac-RLYE with CPT-11 or other chemotherapeutic drugs

Molecular Pharmacology Fast Forward. Published on October 8, 2019 as DOI: 10.1124/mol.119.117234
This article has not been copyedited and formatted. The final version may differ from this version.

is a potential approach in the treatment of cancer via increased TAM-induced tumor cytotoxicity.

Macrophages isolated from tumor-bearing mice express both VEGFR-1 and VEGFR-2, whereas macrophages harvested from non-tumor-bearing animals express only VEGFR-1 (Dineen et al., 2008), suggesting that VEGFR-2 is essential for macrophage infiltration into tumors. Indeed, the monoclonal antibody against VEGFR-2, ramucirumab, is clinically used for treating patients with different tumor types (Aprile et al., 2014). This suggests that the specific blockade of VEGFR-2 activation might be more effective than other anti-angiogenic strategies, including VEGFR-2 kinase inhibitors with relatively low specificity (Cook and Figg, 2010; Verheul and Pinedo, 2007) and anti-VEGF antibodies with several side effects (Kamba and McDonald. 2007; Taugourdeau-Raymond et al., 2012). Thus, specific inhibitors of VEGFR-2 overcome not only tumor angiogenesis, but also tumor immune privilege, without serious systemic toxicity (Roland et al., 2009). Our data showed that Ac-RLYE, an N-terminal acetylated peptide of RLYE specifically bound to VEGFR-2 (Beak et al., 2017), potentially inhibited infiltration of macrophages into tumors and their polarization to the M2 phenotype, which exerts angiogenic and immunosuppressive activities (Riabov et al., 2014). These findings suggest that Ac-RLYE is a potential agent for preventing TAM-mediated creation of unfavorable tumor microenvironment, resulting in enhanced tumor cytotoxicity and decreased tumor angiogenesis.

In conclusion, the present study demonstrates that N-terminal acetylation significantly potentiated the effect of RLYE on angiogenesis, vascular normalization, and tumor immunity in solid tumors, due to its increased serum stability. As a result, Ac-RLYE effectively inhibited tumor progression both by inhibiting tumor angiogenesis and by improving tumor immunity and drug delivery in combination therapy with anticancer drugs. Together, our findings provide

Molecular Pharmacology Fast Forward. Published on October 8, 2019 as DOI: 10.1124/mol.119.117234
This article has not been copyedited and formatted. The final version may differ from this version.

evidence that Ac-RLYE can be used as a potential VEGFR-2 antagonist for anti-angiogenic tumor therapy and enhanced chemotherapeutic drug delivery and efficacy.

Conflicts of interest

The authors declare no conflict of interest.

Author contributions

Participated in research design: J-.A.Y., J.K., Y-.Y.B., Y-.M.K.

Conducted experiments: J-.A.Y, J.K., Y-.Y.B.

Contributed new reagents or analytic tools: D.J., H.L., M-.H.W., K-.S.H., Y-.G.K.

Performed data analysis: W.P., M.P., S.K., T.K., S.C., J-.Y.K.

Wrote or contributed to the writing of the manuscript: J-.A.Y., J.K., Y-.M.K.

References

Agrawal V, Maharjan S, Kim K, Kim NJ, Son J, Lee K, Choi HJ, Rho SS, Ahn S, Won MH, et al. (2014) Direct endothelial junction restoration results in significant tumor vascular normalization and metastasis inhibition in mice. *Oncotarget* 5:2761-2777.

Aprile G, Rijavec E, Fontanella C, Rihawi K and Grossi F. (2014) Ramucirumab: preclinical research and clinical development. *Onco Targets Ther* 7:1997-2006.

Baek YY, Lee DK, Kim J, Kim JH, Park W, Kim T, Han S, Jeoung D, You JC, Lee H, et al. (2017) Arg-Leu-Tyr-Glu tetrapeptide inhibits tumor progression by suppressing angiogenesis and vascular permeability via VEGF receptor-2 antagonism. *Oncotarget* 8:11763-11777.

Baek YY, Lee DK, So JH, Kim CH, Jeoung D, Lee H, Choe J, Won MH, Ha KS, Kwon YG and Kim YM. (2015) The tetrapeptide Arg-Leu-Tyr-Glu inhibits VEGF-induced angiogenesis. *Biochem Biophys Res Commun* 463:532-537.

Carmeliet P and Jain RK. (2011) Principles and mechanisms of vessel normalization for cancer and other angiogenic diseases. *Nat Rev Drug Discov* 10:417-427.

Charan J and Kantharia ND. (2013) How to calculate sample size in animal studies? *J Pharmacol Pharmacother* 4:303-306.

Cook KM and Figg WD. (2010) Angiogenesis inhibitors: current strategies and future prospects. *CA Cancer J Clin* 60:222-243.

De Palma M and Lewis CE. (2013) Macrophage regulation of tumor responses to anticancer therapies. *Cancer Cell* 23:277-286.

Dickson PV, Hamner JB, Sims TL, Fraga CH, Ng CY, Rajasekeran S, Hagedorn NL, McCarville MB, Stewart CF and Davidoff AM. (2007) Bevacizumab-induced transient remodeling of the vasculature in neuroblastoma xenografts results in improved delivery and efficacy of systemically administered chemotherapy. *Clin Cancer Res* 13:3942-3950.

Dineen SP, Lynn KD, Holloway SE, Miller AF, Sullivan JP, Shames DS, Beck AW, Barnett CC, Fleming JB and Brekken RA. (2008) Vascular endothelial growth factor receptor 2 mediates macrophage infiltration into orthotopic pancreatic tumors in mice. *Cancer Res* 68:4340-4346.

Folkman J. (2007) Angiogenesis: an organizing principle for drug discovery? *Nat Rev Drug Discov* 6:273-286.

Fuchs CS, Tomasek J, Yong CJ, Dumitru F, Passalacqua R, Goswami C, Safran H, Dos Santos LV, Aprile G, Ferry DR, et al. (2014) REGARD Trial Investigators, Ramucirumab monotherapy for previously treated advanced gastric or gastro-oesophageal junction adenocarcinoma (REGARD): an international, randomised, multicentre, placebo-controlled, phase 3 trial. *Lancet* 383:31-39

Hellström M, Gerhardt H, Kalén M, Li X, Eriksson U, Wolburg H and Betsholtz C. (2001) Lack of pericytes leads to endothelial hyperplasia and abnormal vascular morphogenesis. *J*

Cell Biol 153:543-553.

Hicklin DJ and Ellis LM. (2005) Role of the vascular endothelial growth factor pathway in tumor growth and angiogenesis. *J Clin Oncol* 23:1011-1127.

Hughes R, Qian BZ, Rowan C, Muthana M, Keklikoglou I, Olson OC, Tazzyman S, Danson S, Addison C, Clemons M, et al. (2015) Perivascular M2 macrophages stimulate tumor relapse after chemotherapy. *Cancer Res* 75:3479-3491.

Javle M, Smyth EC and Chau I. (2014) Ramucirumab: successfully targeting angiogenesis in gastric cancer. *Clin Cancer Res* 20:5875-5881.

Jain RK. (2005) Normalization of tumor vasculature: an emerging concept in antiangiogenic therapy. *Science* 307:58-62.

Kamba T and McDonald DM. (2007) Mechanisms of adverse effects of anti-VEGF therapy for cancer. *Br J Cancer* 96:1788-1795.

Kerbel RS. (2008) Tumor angiogenesis. *N Engl J Med* 358:2039-2049.

Lee JH, Cho HS, Lee JJ, Jun SY, Ahn JH, Min JS, Yoon JY, Choi MH, Jeon SJ, Lim JH, et al. (2016) Plasma glutamate carboxypeptidase is a negative regulator in liver cancer metastasis. *Oncotarget* 7:79774-79786.

Leppänen VM, Prota AE, Jeltsch M, Anisimov A, Kalkkinen N, Strandin T, Lankinen H, Goldman A, Ballmer-Hofer K and Alitalo K. (2010) Structural determinants of growth factor binding and specificity by VEGF receptor 2. *Proc Natl Acad Sci USA* 107:2425-2430.

Margonis GA, Buettner S, Andreatos N, Sasaki K, Pour MZ, Deshwar A, Wang J, Ghasebeh MA, Damaskos C, Rezaee N, et al. (2017) Preoperative bevacizumab and volumetric recovery after resection of colorectal liver metastases. *J Surg Oncol* 116:1150-1158.

Martinez-Martos JM, del Pilar Carrera-Gonzalez M, Duenas B, Mayas MD, Garcia MJ and Ramírez-Exposito MJ. (2011) Renin angiotensin system-regulating aminopeptidase activities in serum of pre- and postmenopausal women with breast cancer. *Breast* 20:444-447.

Mazibrada J, Rittà M, Mondini M, De Andrea M, Azzimonti B, Borgogna C, Ciotti M, Orlando

A, Surico N, Chiusa L, et al. (2008) Interaction between inflammation and angiogenesis during different stages of cervical carcinogenesis. *Gynecol Oncol* 108:112-120.

McDonald DM and Baluk P. (2005) Imaging of angiogenesis in inflamed airways and tumors: newly formed blood vessels are not alike and may be wildly abnormal: Parker B. Francis lecture. *Chest* 128:602S-608S.

McIntyre A and Harris AL. (2015) Metabolic and hypoxic adaptation to anti-angiogenic therapy: a target for induced essentiality. *EMBO Mol Med* 7:368-379.

Ohm JE and Carbone DP. (2001) VEGF as a mediator of tumor-associated immunodeficiency. *Immunol Res* 23:263-272.

Ohm JE, Gabrilovich DI, Sempowski GD, Kisseleva E, Parman KS, Nadaf S and Carbone DP. (2003) VEGF inhibits T-cell development and may contribute to tumor-induced immune suppression. *Blood* 101:4878-4886.

Osada T, Chong G, Tansik R, Hong T, Spector N, Kumar R, Hurwitz HI, Dev I, Nixon Ab, Lyerly HK, et al. (2008) The effect of anti-VEGF therapy on immature myeloid cell and dendritic cells in cancer patients. *Cancer Immunol Immunother* 57:1115-1124.

Ozerdem U, Grako KA, Dahlin-Huppe K, Monosov E and Stallcup WB. (2001) NG2 proteoglycan is expressed exclusively by mural cells during vascular morphogenesis. *Dev Dyn* 222:218-227.

Papetti M and Herman IM (2002) Mechanisms of normal and tumor-derived angiogenesis. *Am J Physiol Cell Physiol* 282:947-970.

Rahma OE and Hodi FS. (2019) The Intersection between Tumor Angiogenesis and Immune Suppression. *Clin Cancer Res* [Epub ahead of print]

Riabov V, Gudima A, Wang N, Mickley A, Orekhov A and Kzhyshkowska J. (2014) Role of tumor associated macrophages in tumor angiogenesis and lymphangiogenesis. *Front Physiol* 5:75.

Rivera LB and Bergers G. (2015) Tumor angiogenesis, from foe to friend. *Science* 349:694-695.

Roland CL, Lynn KD, Toombs JE, Dineen SP, Udugamasooriya DG and Brekken RA. (2009) Cytokine levels correlate with immune cell infiltration after anti-VEGF therapy in preclinical mouse models of breast cancer. *PLoS One* 4:e7669.

Sawano A, Takahashi T, Yamaguchi S, Aonuma T and Shibuya M. (1996) Flt-1 but not KDR/Flk-1 tyrosine kinase is a receptor for placenta growth factor, which is related to vascular endothelial growth factor. *Cell Growth Diff* 7:213-221.

Sengupta S, Rojas R, Mahadevan A, Kasper E and Jeyapalan S. (2015) CPT-11/bevacizumab for the treatment of refractory brain metastases in patients with HER2-neu-positive breast cancer. *Oxf Med Case Reports* 2015:254-257.

Sheppard GS, Kawai M, Craig RA, Davidson DJ, Majest SM, Bell RL and Henkin J. (2004) Lysyl 4-aminobenzoic acid derivatives as potent small molecule mimetics of plasminogen kringle 5. *Bioorg Med Chem Lett* 14:965-966.

Shibuya M. (2011) Vascular endothelial growth factor (VEGF) and its receptor (VEGFR) signaling in angiogenesis: A crucial target for anti- and pro-angiogenic therapies. *Genes Cancer* 2:1097-1105.

Shrimali RK, Yu Z, Theoret MR, Chinnasamy D, Restifo NP and Rosenberg SA. (2010) Antiangiogenic agents can increase lymphocyte infiltration into tumor and enhance the effectiveness of adoptive immunotherapy of cancer. *Cancer Res* 70:6171-6180.

Taugourdeau-Raymond S, Rouby F, Default A and Jean-Pastor MJ. (2012) French Network of Pharmacovigilance Centers. Bevacizumab-induced serious side-effects: a review of the French pharmacovigilance database. *Eur J Clin Pharmacol* 68:1103-1107.

Terme M, Pernot S, Marcheteau E, Sandoval F, Benhamouda N, Colussi O, Dubreuil O, Carpentier AF, Tartour E and Taieb J. (2013) VEGFA-VEGFR pathway blockade inhibits tumor-induced regulatory T-cell proliferation in colorectal cancer. *Cancer Res* 73:539-549.

Uchino J, Takayama K, Harada A, Sone T, Harada T, Curiel DT, Kuroki M and Nakanishi Y. (2008) Tumor targeting carboxylesterase fused with anti-CEA scFv improve the anticancer effect with a less toxic dose of irinotecan. Cancer Gene Ther 15:94-100.

Verheul HM and Pinedo HM. (2007) Possible molecular mechanisms involved in the toxicity

of angiogenesis inhibition. *Nat Rev Cancer* 7:475-485.

Voron T, Colussi O, Marcheteau E, Pernot S, Nizard M, Pointet AL, Latreche S, Bergaya S, Benhamouda N, Tanchot C, et al. (2015) VEGF-A modulates expression of inhibitory checkpoints on CD8+ T cells in tumors. *J Exp Med* 212:139-148.

Wheeler KC, Jena MK, Pradhan BS, Nayak N, Das S, Hsu CD, Wheeler DS, Chen K and Nayak NR. (2018) VEGF may contribute to macrophage recruitment and M2 polarization in the decidua. *PLoS One* 13:e0191040.

Wu X, Giobbie-Hurder A, Liao X, Connelly C, Connolly EM, Li J, Manos MP, Lawrence D, McDermott D, Severgnini M, et al. (2017) Angiopoietin-2 as a biomarker band target for immune checkpoint therapy. *Cancer Immunol Res* 5:17-28.

Yanagisawa M, Yorozu K, Kurasawa M, Nakano K, Furugaki K, Yamashita Y, Mori K and Fujimoto-Ouchi K. (2010) Bevacizumab improves the delivery and efficacy of paclitaxel. *Anticancer Drugs* 21:687-694.

Zhao Y, Zhang C, Gao L, Yu X, Lai J, Lu D, Bao R, Wang Y, Jia B, Wang F, et al. (2017) Chemotherapy-induced macrophage infiltration into tumors enhances nanographene-based photodynamic therapy. *Cancer Res* 77:6021-6032.

Zhong WQ, Chen G, Zhang W, Xiong XP, Zhao Y, Liu B and Zhao YF. (2015) M2-polarized macrophages in keratocystic odontogenic tumor: relation to tumor angiogenesis. *Sci Rep* 5:15586.

Footnotes

This work was supported by the National Research Foundation of Korea (NRF) Grant funded by the Korea Government (MSIP) (NRF-2017R1A2B3004565).

Molecular Pharmacology Fast Forward. Published on October 8, 2019 as DOI: 10.1124/mol.119.117234
This article has not been copyedited and formatted. The final version may differ from this version.

Figure Legends

Fig. 1. RLYE is degraded by a heat-labile serum factor. (A) Chemical structure of RLYE. (B) RLYE was incubated with PBS or healthy human serum at 37°C for the indicated time periods. The reaction mixture was fractionated by reverse-phase HPLC, and peptide concentration was analyzed by the integration of absorbance at 220 nm as a function of retention (n =3). Inserted peaks show a typical chromatogram of RLYE that was incubated in fresh human serum for the indicated times. (C) Human serum was pre-heated at the indicated temperature for 10 min and then incubated with RLYE at 37°C for 2 h. Representative spectra of the remaining RLYE were obtained via HPLC-based analysis.

Fig. 2. Degradation of RLYE in serum is blocked by inhibitors of aminopeptidases B and N. (A) RLYE was incubated in PBS, human serum, or 50% human albumin solution in the presence or absence of aprotinin (1 μM), EDTA (1 mM), leupeptin (100 μM), or PMSF (1 mM) at 37°C for 4 h. The remaining peptide was determined by HPLC-based analysis. (B) RLYE was incubated in PBS or human serum in the absence or presence of bestatin (50 μM) at 37℃ for 4 h and analyzed by HPLC. (C) The peptide was incubated in PBS or human serum in the absence or presence of arphamenine B (50 μM), leuhistin (50 μM), or a combination of both at 37°C for 4 h and analyzed by HPLC. (A-C) All the peaks are representative spectra of two independent experiments.

Fig. 3. N-terminal modification of RLYE increases stability and anti-angiogenic activity in serum. (A and B) RLYE and its modified derivatives at N- and C-termini were incubated in human serum at 37°C for the indicated time periods. The remaining peptide was determined by HPLC-based analysis (n =3). (C) Half-lives of RLYE and its derivatives were calculated

Molecular Pharmacology Fast Forward. Published on October 8, 2019 as DOI: 10.1124/mol.119.117234
This article has not been copyedited and formatted. The final version may differ from this version.

from data of the panels A and B (n = 3). The inhibitory effects of RLYE (1.5 nM) and its derivatives on angiogenesis were determined by assaying chemotactic migration of HUVECs stimulated with 10 ng/ml of VEGF-A (n = 3). The IC_{50} values and their 95% confidence intervals (95% CI) against endothelial cell migration were determined by (Supplementary Fig. 1) plotting the pooled data from three independent experiments performed in triplicated using the logarithmic regression. **P* <0.05 vs. RLYE. (D) RLYE and its derivatives were pre-incubated in PBS or human serum for 2 h, followed by assessment of their inhibitory activity against VEGF-A-induced tube formation of HUVECs. Scale bar = 250 μm. Tube length was measured using ImageJ software, and data were analyzed using two-way ANOVA followed by Tukey's post-hoc test (n = 3). ns = not significant. ***P* <0.01.

Fig. 4. Ac-RLYE and $R_{(D)}$LYE inhibit tumor angiogenesis and growth. Nude mice were challenged s.c. in the left flank with 1×10^7 HCT116 human colon carcinoma cells in a volume of 100 μl. On day 6 when the tumor volume reached 50-70 mm^3, mice were i.p. injected with saline, RLYE (0.5 mg/kg daily), or modified RLYEs (0.5 mg/kg daily) for 24 days (n = 6). (A) Tumor burden was measured by three blinded observers every 3 days. The arrow indicates the beginning of the peptide treatment. (B) The size of tumors excised from HCT116 tumor-bearing mice treated with peptides for 24 days (n =6). (C) Tumor weight was measured immediately after isolation (n = 6). (D) Representative image of tumor sections that were stained with an anti-CD31 antibody. Scale bar = 100 μm. (E) CD31 levels were quantified by three blinded observers using computer-aided confocal microscopy. Data were analyzed using one-way ANOVA followed by Tukey's post-hoc test (n = 6). ns = not significant. **P* < 0.05 and ***P* < 0.01.

Fig. 5. Ac-RLYE improves tumor vessel normalization. HCT116 tumor-bearing mice were i.p. injected daily with saline, RLYE (0.5 mg/kg), or Ac-RLYE (0.5 mg/kg) for 18 days. (A and B) Vascular permeability was assessed and quantified in tumor tissues from mice after 10 min of i.v. injection with FITC-dextran using computer-aided confocal microscopy (n = 8). (C) Representative immunofluorescence staining images showing CD31 and VE-cadherin in the tumor sections, and (D) the ratio of VE-cadherin to CD31 was quantified using computer-aided confocal microscopy (n = 8). (E) Representative immunofluorescence staining images showing CD31 and NG2 in the tumor sections, and (F) Pericyte coverage was quantified as a percentage of $NG2^+$-covered area that lies along the $CD31^+$-blood vessels (n = 8). (B, D, and F) Statistical analysis was performed using one-way ANOVA followed by Tukey's post hoc test (n = 8). All scale bars = 100 μm. $^{**}P < 0.01$.

Fig. 6. Ac-RLYE improves chemosensitivity of tumors. HCT116 tumor-bearing mice were i.p. injected with RLYE (0.5 mg/kg daily) or Ac-RLYE (0.5 mg/kg daily) alone or in combination with irinotecan (CPT-11 or CPT, 17 mg/kg every 5 days). The arrow indicates the beginning of peptide and CPT-11 treatment. (A) Tumor volumes were measured every 3 days (n = 11). (B and C) Apoptotic cells in tumor tissues were determined and quantified using TUNEL assay (n = 11). (D) The levels of alanine aminotransferase (ALT) and aspartate aminotransferase (AST) were determined in serum from mice at the end of experiment using a colorimetric assay kit (Asan Pharmaceutical, Seoul, Korea). Scale bar = 100 μm in all images. ns = not significant. $^{**}P < 0.001$.

Fig. 7. Ac-RLYE attenuates polarization of TAMs to M2 phenotype. Tumors isolated from HCT116 tumor-bearing mice folloeing treatment with Ac-RLYE, CPT-11, or a combination of

Molecular Pharmacology Fast Forward. Published on October 8, 2019 as DOI: 10.1124/mol.119.117234
This article has not been copyedited and formatted. The final version may differ from this version.

both, were immunostained with antibodies against F4/80, Arg1, or iNOS. (A) Representative images for F4/80 and Arg1 were obtained using computer-aided confocal microscopy. (B) $F4/80^+$ TAMs were quantified by examining eight high-power fields (HPFs) per slide (n = 11). (C) $F4/80^+Arg^+$ cells were also quantified (n = 11). (D) Representative images for F4/80 and iNOS were obtained using computer-aided confocal microscopy. (E) $F4/80^+iNOS^+$ cells were quantified (n = 11). (F) The ratio of M1 and M2 was calculated from the relative levels of $F4/80^+Arg^+$ cells and $F4/80^+iNOS^+$ cells (n = 11). Scale bars, 100 μm. *$P < 0.05$ and ** $P < 0.001$.

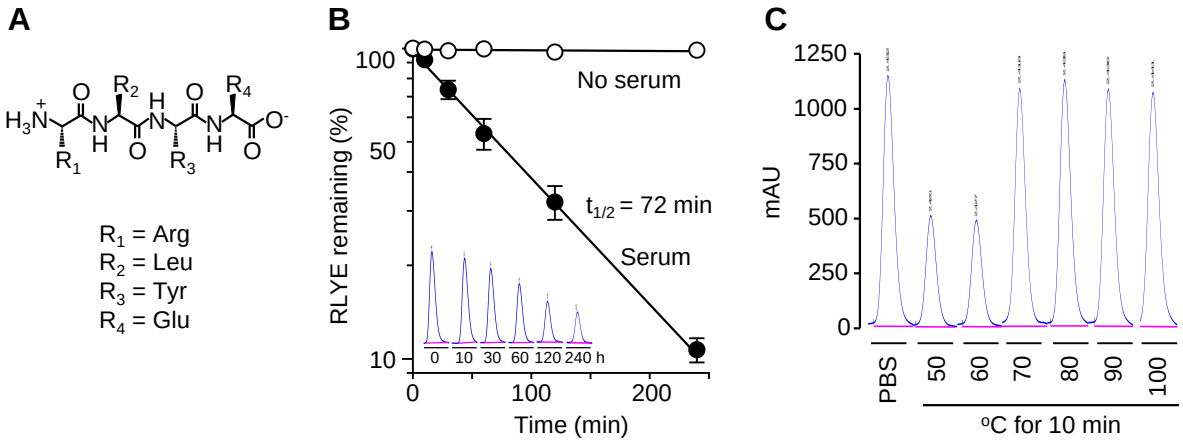
A
B
C
R1 = Arg
R2 = Leu
R3 = Tyr
R4 = Glu
RLYE remaining (%)
100
50
10
No serum
t1/2 = 72 min
Serum
0 10 30 60 120 240 h
0
100
200
Time (min)
mAU
1250
1000
750
500
250
0
PBS
50
60
70
80
90
100
oC for 10 min

Figure 1

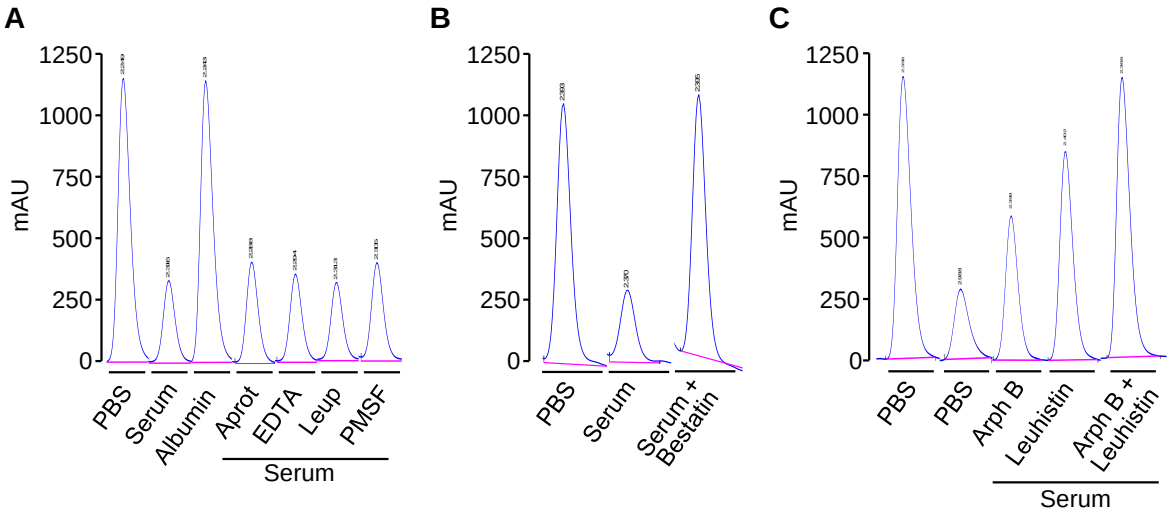
A
B
C
mAU
1250
1000
750
500
250
0
PBS
Serum
Albumin
Aprot
EDTA
Leup
PMSF
Serum
Serum + Bestatin
Arph B
Leuhistin
Arph B + Leuhistin

Figure 2

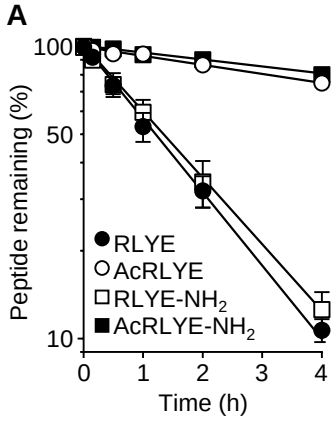

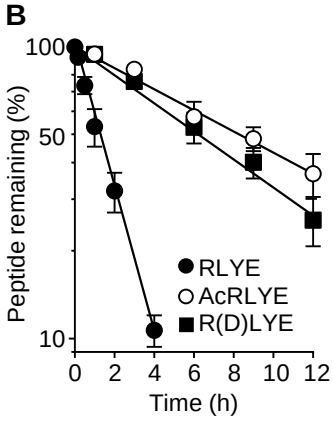

C

Peptides	$t_{1/2}$ (h)	Angiogenic inhibition (%)	IC_{50} (95% CI) pM
RLYE	1.2	85.4±2.5	89.1 (69.1–116.9)
AcRLYE	8.8	95.8±3.8*	37.1 (30.9–44.7)
RLYE-NH_2	1.3	79.7±4.1	326.6 (224.8–475.3)
AcRLYE-NH_2	9.4	11.3±2.7	>1,000
$R_{(D)}$LYE	7.0	91.4±4.3	52.5 (39.8–70.8)

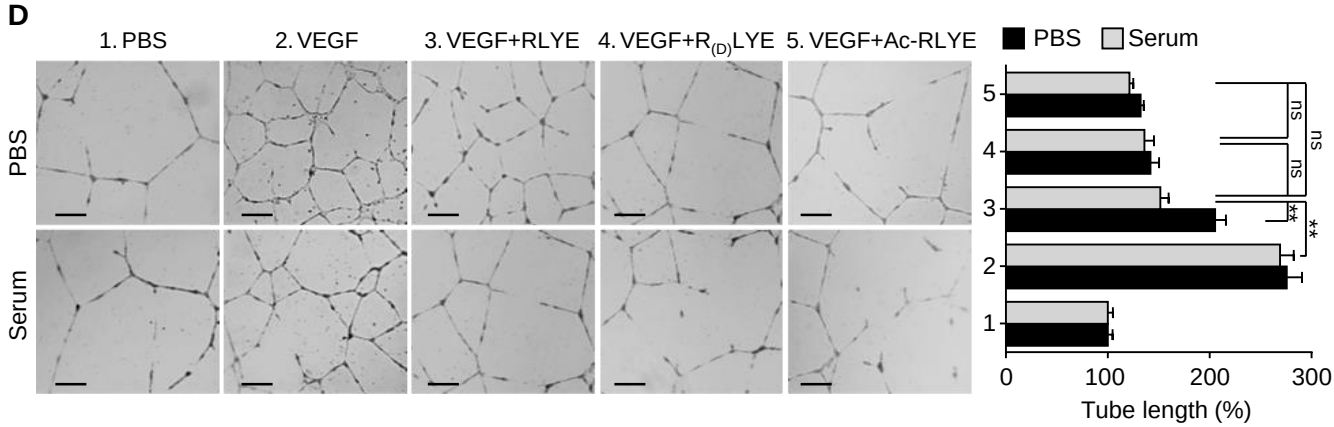

Figure 3

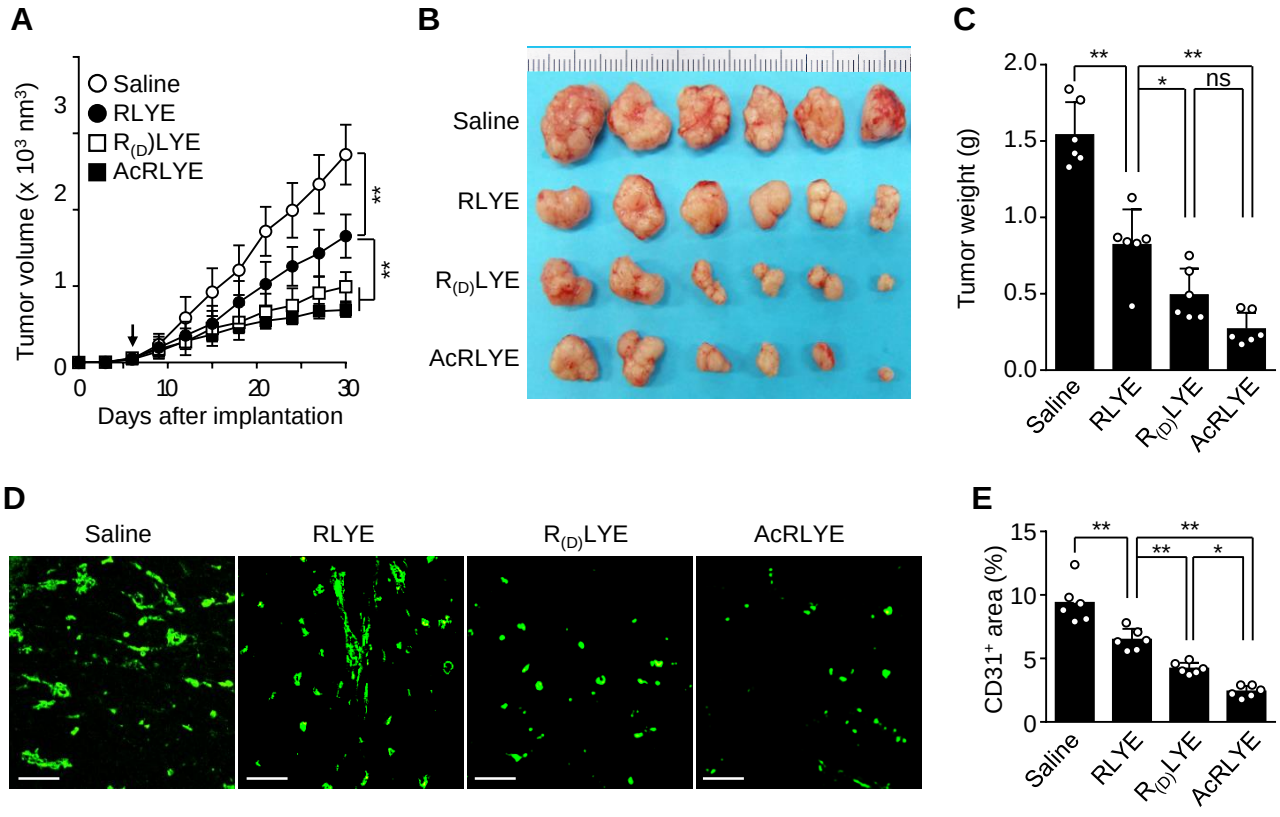
A
Saline
RLYE
R(D)LYE
AcRLYE
Tumor volume (x 10³ nm³)
Days after implantation
**
**
B
Saline
RLYE
R(D)LYE
AcRLYE
C
Tumor weight (g)
**
**
*
ns
Saline
RLYE
R(D)LYE
AcRLYE
D
Saline
RLYE
R(D)LYE
AcRLYE
E
CD31⁺ area (%)
**
**
**
*
Saline
RLYE
R(D)LYE
AcRLYE

Figure 4

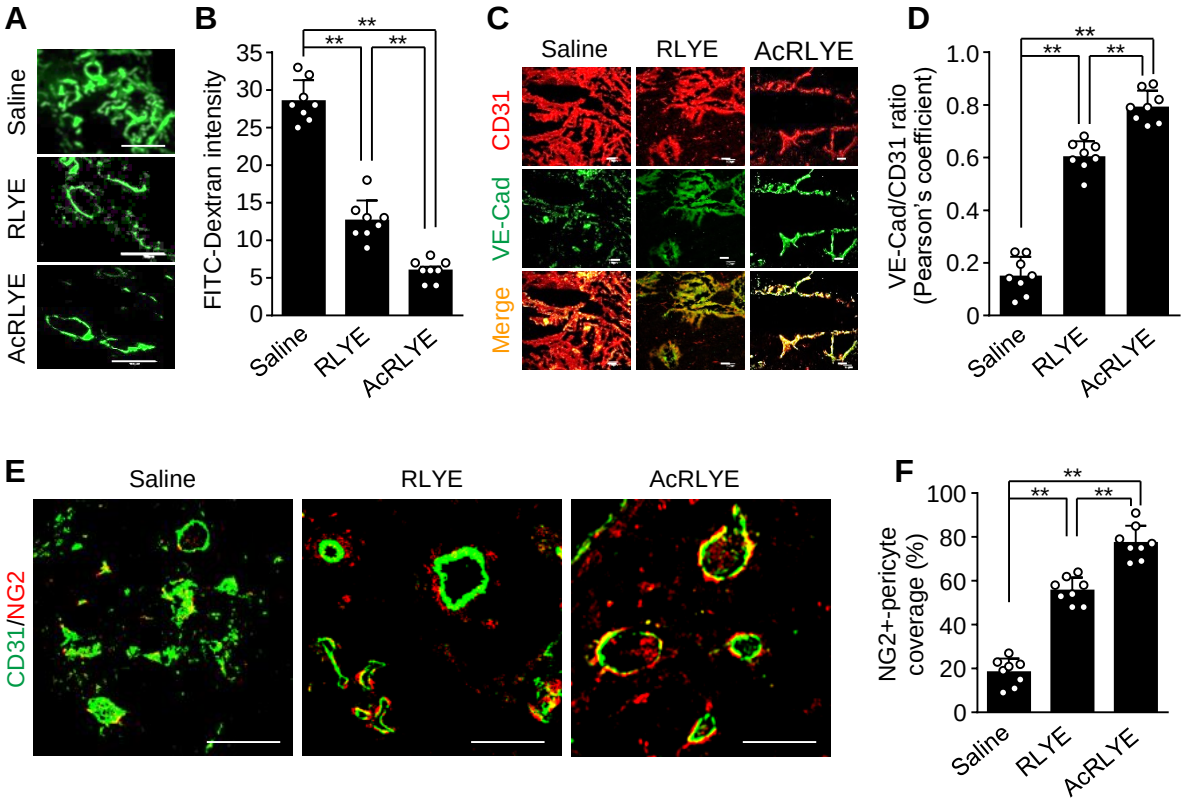
A
Saline
RLYE
AcRLYE
B
FITC-Dextran intensity
35
30
25
20
15
10
5
0
**
**
**
Saline
RLYE
AcRLYE
C
Saline
RLYE
AcRLYE
CD31
VE-Cad
Merge
D
VE-Cad/CD31 ratio
(Pearson's coefficient)
1.0
0.8
0.6
0.4
0.2
0
**
**
**
Saline
RLYE
AcRLYE
E
Saline
RLYE
AcRLYE
CD31/NG2
F
NG2+-pericyte
coverage (%)
100
80
60
40
20
0
**
**
**
Saline
RLYE
AcRLYE

Figure 5

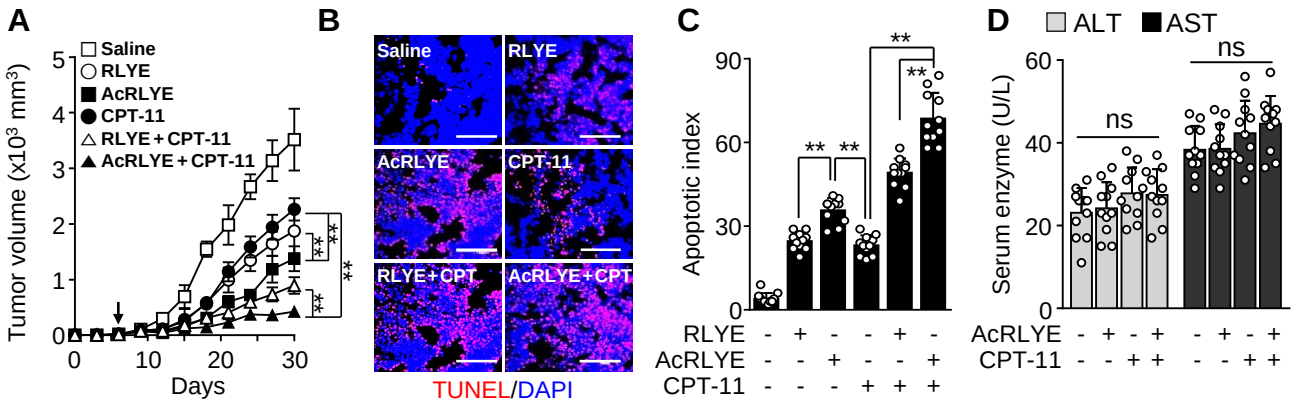
A
B
C
D
Saline
RLYE
AcRLYE
CPT-11
RLYE + CPT-11
AcRLYE + CPT-11
Tumor volume (x10³ mm³)
Days
TUNEL/DAPI
Apoptotic index
RLYE
AcRLYE
CPT-11
ALT
AST
Serum enzyme (U/L)
ns

Figure 6

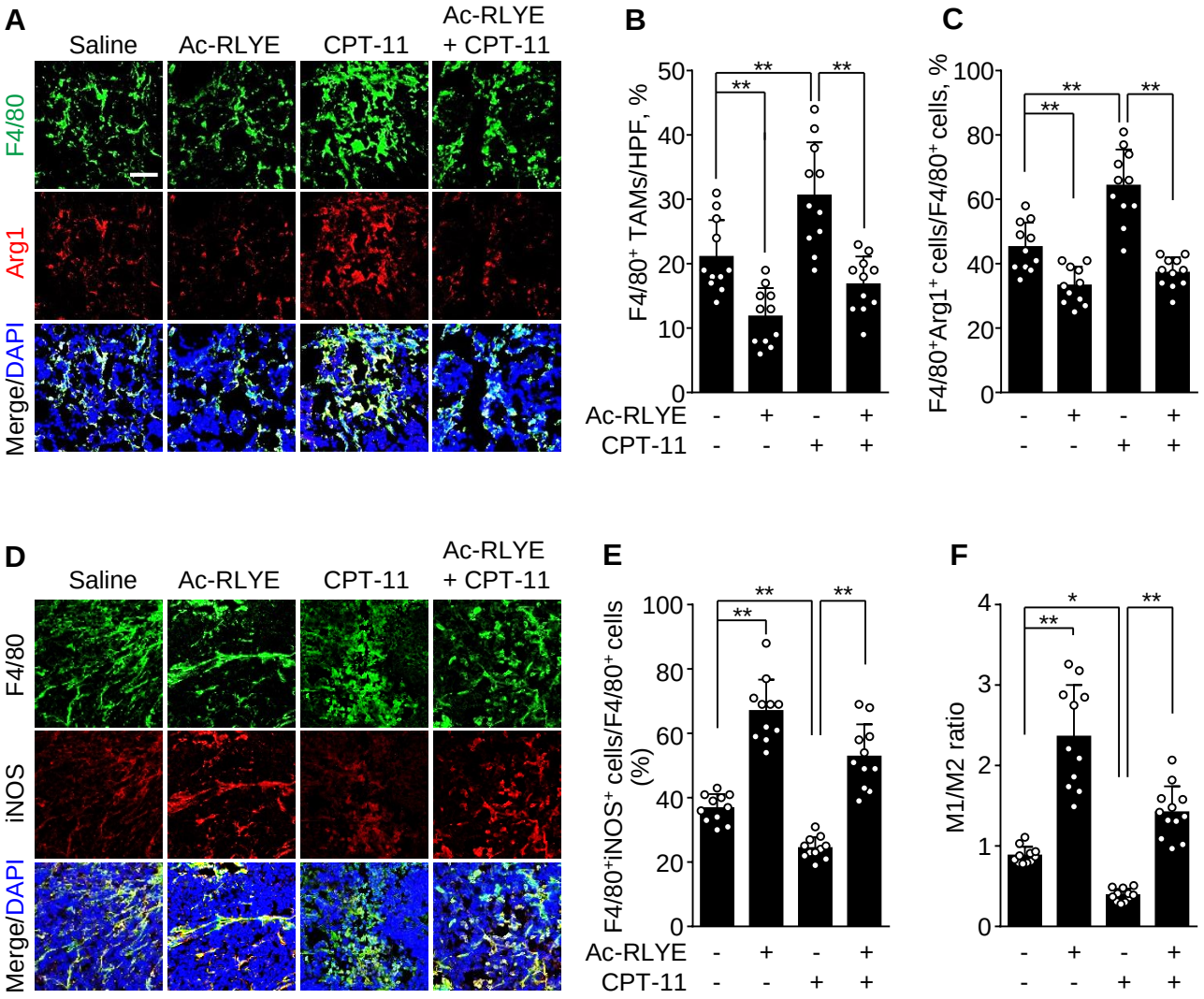
A
Saline
Ac-RLYE
CPT-11
Ac-RLYE + CPT-11
F4/80
Arg1
Merge/DAPI
B
F4/80⁺ TAMs/HPF, %
Ac-RLYE
CPT-11
C
F4/80⁺Arg1⁺ cells/F4/80⁺ cells, %
D
Saline
Ac-RLYE
CPT-11
Ac-RLYE + CPT-11
F4/80
iNOS
Merge/DAPI
E
F4/80⁺iNOS⁺ cells/F4/80⁺ cells (%)
F
M1/M2 ratio

Figure 7